

Near-Field Probing Surface Plasmon Enhancement Effect on Two-Photon Emission

Yuzhen Shen, Jacek Swiatkiewicz, Tzu-Chau Lin, Przemyslaw Markowicz, and Paras N. Prasad*

Photonics Research Laboratory, Institute for Lasers, Photonics and Biophotonics, Departments of Chemistry, Physics, Electrical Engineering, and Medicine, University at Buffalo, The State University of New York, Buffalo, New York 14260

Received: December 20, 2001; In Final Form: March 1, 2002

A photon scanning tunneling microscope is employed to probe the surface-plasmon-induced local field enhancement effect on two-photon fluorescence from organic nanoparticles adsorbed on silver surface. A size dependence of fluorescence enhancement and photodecomposition is observed, which results from the competition between the surface-plasmon-enhanced two-photon fluorescence and the nonradiative energy transfer from the excited dye molecules to the silver surface.

A surface-plasmon (SP) is a localized electromagnetic field at metal-dielectric interfaces.^{1,2} The field associated with SP is sensitive to the variations in the environment adjacent to the interfaces and therefore has potential as a sensing probe.³ The field enhancement due to SP resonance is predicted to be $\sim 10^2$ times larger than the incident field,² and therefore can be used to increase nonlinear optical effects at interfaces.^{4–9} The SP-induced electromagnetic field is evanescent, and is not accessible by far-field SP optics. Furthermore, the resolution in far-field SP optics is limited to SP decay length, and the information about spatial structures obtained by far-field SP optics is the average response over a macroscopic region. The advances in near-field scanning optical microscopy (NSOM)^{10–13} and photon scanning tunneling microscopy (PSTM)^{14–18} makes it possible to perform direct measurements on SP in the near field and probe SP related effects on a nanoscopic region. The principle of NSOM is to scan a nanoscopic light source in the near field above a sample with the resulting field intensity being detected. With PSTM, a nanoscopic probe senses the evanescent field above the sample that is illuminated under attenuated total reflection (ATR). Because SP can be excited by evanescent wave arising from ATR, ATR-based PSTM has potential benefit in near-field SP studies. Recently, PSTM has been used to detect SP resonance in randomly rough surface, fractal colloid clusters, continuous metal film, and single metal particles.^{19–24} However, there is no attempt to apply SP resonance to near-field nonlinear fluorescence study. In this letter, we employ PSTM to probe SP-induced local field enhancement and apply the enhancement effect to near-field two-photon fluorescence imaging and spectroscopic study on organic nanoparticles.

The schematic of the experimental setup is shown in Figure 1. A self-mode-locked Ti:Sapphire laser (Coherent) is used as an excitation source at 800 nm with an average power of 2 W. The pulse width is 80 fs at a repetition rate of 80 MHz. The laser output is passed through a polarizer, focused by a lens, then incident on the sample that is mounted with an index matching oil on a BK7 prism under total internal reflection. Position lens L and align mirror M so that the sample surface lies in the focal plane and the incident beam that is parallel to the optical axis of the lens L is refracted through the focus at a different angle when mirror M is scanned up and down. As a

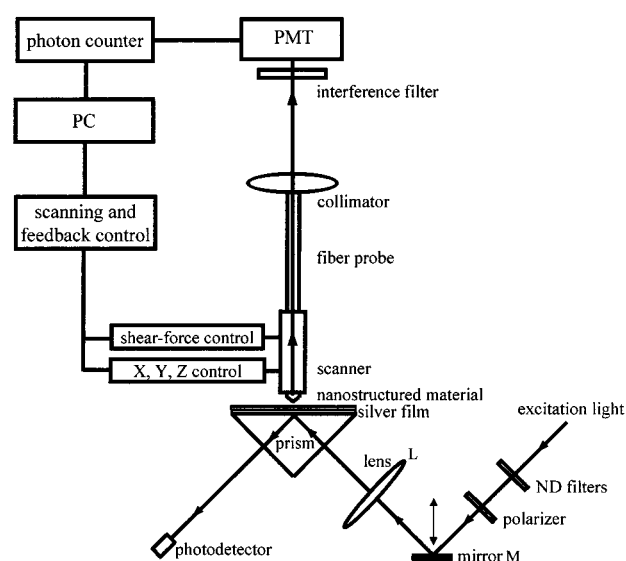


Figure 1. Schematic of the experimental setup.

result, the angle of incidence can be adjusted by scanning mirror M in increments of 0.085 mm without changing focus point on the sample, which corresponds to 0.05° each step. The dynamic range of angular scan is $\sim 10^\circ$. The reflected light intensity is detected with a photodiode to measure SP resonance curve. The transmission or fluorescence signal is collected by an aluminum-coated fiber probe (Topometrix) with an aperture of 50 nm in the near-field above the sample, passed through band-pass filter, and detected by a cooled photomultiplier (Hamamatsu) connected to photon-counting electronics (Stanford Research System) and a computer to process data or generate optical image. Shear-force feedback that uses tuning-fork detection monitors the oscillation of the probe, and keeps the probe-sample separation constant. A Shear-force image can be produced simultaneously with the optical image, as the probe is rastered across the sample surface.

A silver film of 50 nm is evaporated on half of a BK7 microscope cover glass at 10^{-6} Torr and then used as a sample. The excitation light is transmitted through the silver film as an exponentially decaying wave, which is localized at silver surface and can be detected only in the near-field. To measure the SP-

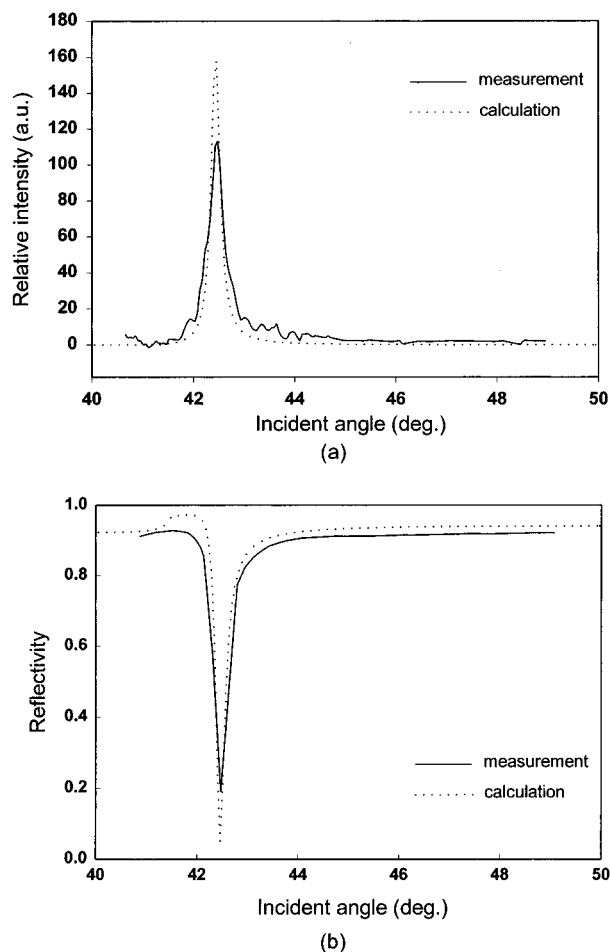


Figure 2. (a) SP-induced local field enhancement and (b) SP resonance curve.

induced local field enhancement, the probe is held stationary in the near-field above a local site of silver film, while detecting the transmitted intensity with varying the angle of incidence. Figure 2(a) shows the angular dependence of transmitted field intensity, and Figure 2(b) shows the angular reflectivity. The intensity of transmitted field reaches a maximum while the intensity of reflected field is at a minimum, indicating the resonance excitation of surface plasmon. The enhancement of local field intensity due to SP resonance is by a factor of 122 with respect to the intensity off resonance. The same measurement is repeated at different locations and shows slight difference in enhancement factor. Simulation of SP-induced local field enhancement and SP reflectance curve as a function of incident angle is also performed for a comparison with the experimental data, and is shown in Figure 2(a) and 2(b), respectively, which is in good agreement with the measurement. The calculation is based on Fresnel equations² for prism-metal film-air configuration. The difference in enhancement factor and reflectivity between the measurement and the calculation could be due to the spectral width of femtosecond pulses and the focused laser beam as compared to a collimated monochromatic plane wave. As a result, the excitation light is partially converted into the SP, and the effective SP coupling efficiency decreases. The field intensity of the evanescent wave on the bare glass is also measured. The ratio of the transmitted field intensity in the presence and absence of silver overlayer is ~ 22 , close to our theoretical prediction, in which the ratio of 31.2 is obtained.

The physical origin of the local field enhancement can be related to collective charge oscillation. The resonance enhance-

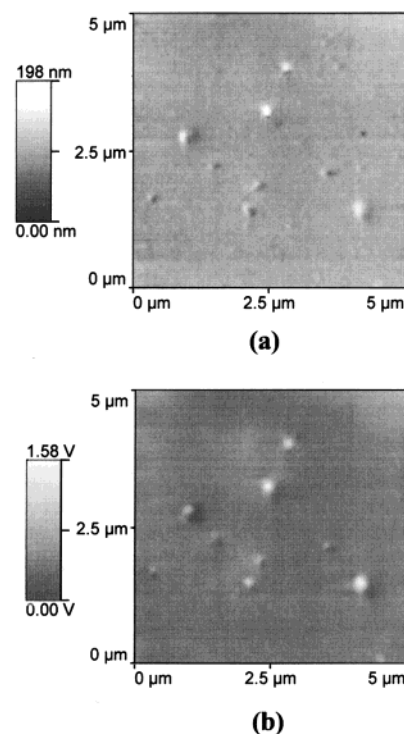


Figure 3. (a) Shear-force image and (b) SP-enhanced two-photon fluorescence image of PRL-701 particles.

ment effect is then applied to near-field two-photon fluorescence imaging and spectroscopic study on organic nanoparticles. The sample used before is mapped with shear-force detection, which indicates that no tiny cluster islands are observed on the metallic film. The sample is then removed from the prism and spin coated with a drop of dilute tetrahydrofuran (THF) solution of N, N, N-tris[4-{2-(4-{5-[4-(*tert*-butyl) phenyl]-1, 3, 4-oxadiazol-2-yl} phenyl)-1-ethenyl} phenyl] amine (abbreviated as PRL-701), which is nanofiltered prior to the deposition on the silver film. PRL-701 is a new two-photon chromophore synthesized at our laboratory, which exhibits a large two-photon excitation cross section at ~ 800 nm.²⁵ Figure 3(a) and 3(b) shows simultaneously collected shear-force image and two-photon fluorescence image, respectively, of isolated PRL-701 nanoparticles at the resonance angle of 43.70° . Due to the presence of PRL-701, the SP resonance angle shifts to a larger value compared to that for bare silver film. The intensity variation of two-photon fluorescence correlated with the topographic features. The full width at half-maximum (fwhm) of the smallest feature in fluorescence image is 108 nm, which is better than $\lambda/7$, where λ is the illumination wavelength. The fwhm of corresponding topographic feature is 120 nm. Some particles of ~ 50 – 60 nm diameter and ~ 30 – 40 nm thickness can be resolved on topographic image, but are not observable on fluorescence image. This is due to the competitive effect arising from the enhanced emission and the quenching by energy transfer from excited molecules to the silver surface. Because nonradiative decay rate decreases as d^{-3} ,²⁶ where d is the distance between the excited molecules and the metal surface, large size particles favor the enhanced emission and fluorescence is not significantly quenched. However, for those smaller size particles that are placed near the silver surface within ~ 40 nm, nonradiative energy transfer is dominant and a substantial fraction of fluorescence is quenched. A similar measurement is also performed, in which nonmetallic substrate is used to eliminate the SP effects. The smaller size particles now fluoresce along with the larger ones and can be observed in PSTM images (not

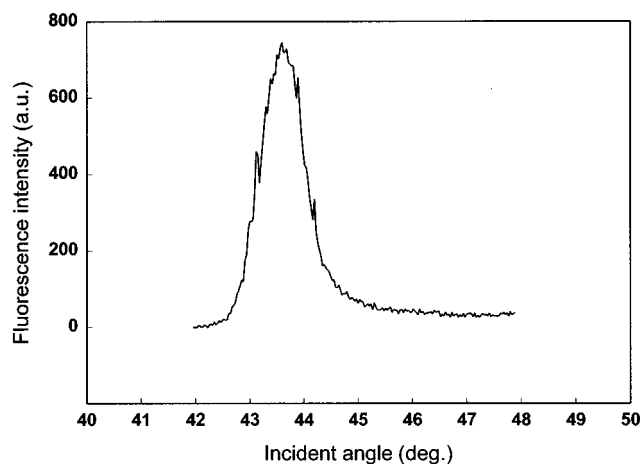


Figure 4. Two-photon fluorescence intensity versus angle of incidence.

shown). This indicates that the smaller particles observed in Figure 3(a) but not visible in Figure 3(b) are not simply dust particles or impurities. The size dependence of fluorescence enhancement and quenching shown in Figure 3 is consistent with the fluorescence lifetime measurement,²⁷ which indicates that the effective fluorescence yield comes out only from the molecules at a certain distance above the metal surface. By using the spacer between fluorophore and metal surface, the photodecomposition of adsorbates may be prevented.

The measurement of two-photon fluorescence enhancement is performed on the PRL-701 particle at the lower-right corner of Figure 3, in which the probe is held stationary in the near-field above the particle and the fluorescence intensity is detected with varying the angle of incidence. Figure 4 shows the two-photon fluorescence intensity as a function of incident angle, which indicates that the variation of fluorescence intensity from the particle adsorbed on the silver film is subject to SP-induced local field enhancement. The fluorescence intensity at SP resonance is ~ 750 times stronger than the background intensity far off SP resonance. The profile of fluorescence enhancement is relatively broader due to the presence of PRL701. Because the fluorescence intensity is approximately proportional to the square of the coupling efficiency for two-photon excitation, fluorescence enhancement of $>10^4$ is expected based on the SP-induced local field enhancement curve. The significant loss in the fluorescence enhancement is not only due to the nonradiative energy transfer to the silver surface but also due to the exponential decay of local field enhancement factor, which is estimated to drop by 42.2% from $d = 5$ nm to $d = 100$ nm. The measurement is also performed to compare the fluorescence intensity from similar size particles coated on the silver film and on the bare glass substrate, and a relative enhancement of ~ 100 is obtained, indicating the higher detection sensitivity of SP resonance PSTM.

In conclusion, we have employed PSTM to detect SP-induced local field enhancement and to image two-photon fluorescence from organic nanoparticles adsorbed on metallic surfaces through fluorescence enhancement. We have demonstrated that a subdiffraction-limited optical resolution can be achieved with SP resonance PSTM. We have also shown that SP resonance

PSTM allows a direct observation of fluorescence enhancement and photodecomposition of fluorophores deposited on metallic surface and this leads to the possibility to study fluorescence energy transfer of adsorbed dye molecules on a nanometric scale. Because the collection efficiency of metal-coated probe is very limited in PSTM, SP resonance enhancement effect is helpful to improve the detection sensitivity and increases the signal-to-noise, and this is especially useful for probing near-field nonlinear optical interactions.

Acknowledgment. The authors would like to thank Mr. Christian Reuster for technical support. This work is supported by the Directorate of Chemistry and Life Science of the Air Force of Scientific Research through the University of Southern California MURI Program and in part by the Polymer Branch of the Air Force Research Laboratory at Dayton, Ohio.

References and Notes

- (1) Wallis, P. F.; Stegeman, G. I. *Electromagnetic Surface Excitations*; Springer-Verlag: Berlin, 1986.
- (2) Raether, H. *Surface Plasmons*; Springer: New York, 1988.
- (3) Knoll, W. *Annu. Rev. Phys. Chem.* **1998**, *49*, 565.
- (4) Moskovits, M. *Rev. Mod. Phys.* **1985**, *57*, 783.
- (5) Tsang, T. Y. F. *Opt. Lett.* **1996**, *21*, 245.
- (6) Kano, H.; Kawata, S. *Opt. Lett.* **1996**, *21*, 1849.
- (7) Shalaev, V. M.; Douketis, C.; Haslett, T. L.; Stuckless, T.; Moskovits, M.; *Phys. Rev. B* **1996**, *57*, 11 193.
- (8) Chen, Q.; Sun, X.; Goddington, I. R.; Goetz, D. A.; Simon, H. J. *J. Opt. Soc. Am. B* **1999**, *16*, 971.
- (9) Sipe, J. E.; Stegeman, G. I. Nonlinear Optical Response of Metal Surfaces. In *Surface Polaritons Electromagnetic Waves at Surfaces and Interfaces*; Agranovich, V. M., Mills, L., Eds.; North-Holland: Amsterdam, 1982.
- (10) Phol, D. W.; Denk, W.; Lanz, M. *Appl. Phys. Lett.* **1984**, *44*, 651.
- (11) Lieberman, K.; Harush, S.; Lewis, A.; Kopelman, R. *Science* **1990**, *247*, 59.
- (12) Betzig, E.; Trautman, J. K.; Harris, T. D.; Weiner, J. S.; Kostelak, R. L.; *Science* **1991**, *251*, 1468.
- (13) Higgins, D. A.; Kerimo, J.; Vanden Bout, D. A.; Barbara, P. F. *J. Am. Chem. Soc.* **1996**, *118*, 4049.
- (14) Reddick, R. C.; Warmack, R. J.; Ferrell, T. L.; *Phys. Rev. B* **1989**, *39*, 767.
- (15) Courjoin, D.; Sarayedine, K.; Spajer, M. *Opt. Commun.* **1989**, *71*, 23.
- (16) De Fornel, F.; Goudonnet, J. P.; Salomon, L.; Lesniewska, E. *SPIE* **1989**, *1139*, 77.
- (17) Tsai, D. P.; Othonos, A.; Moskovits, M. *Appl. Phys. Lett.* **1994**, *64*, 1768.
- (18) Shen, Y.; Swiatkiewicz, J.; Winiarz, J.; Markowicz, P.; Prasad, P. N. *Appl. Phys. Lett.* **2000**, *77*, 2946.
- (19) Adam, P. M.; Salomon, L.; De Fornel, F.; Goudonnet, J. P. *Phys. Rev. B* **1993**, *48*, 2680.
- (20) Marti, O.; Bielefeldt, H.; Hecht, B.; Herminghaus, S.; Leiderer, P.; Mlynek, J. *Opt. Commun.* **1993**, *96*, 225.
- (21) Bozhevolnyi, S.; Smolyaninov, I. I.; Zyats, A. V.; *Phys. Rev. B* **1995**, *51*, 17 916.
- (22) Smolyaninov, I. I.; Mazzoni, D. L.; Davis, C. C. *Phys. Rev. Lett.* **1996**, *73*, 3877.
- (23) Kryukov, A. E.; Kim, Y. K.; Ketterson, J. B. *J. App. Phys.* **1997**, *82*, 5441.
- (24) Zhang, P.; Haslett, T. L.; Douketis, C.; Moskovits, M.; *Phys. Rev. Lett.* **1994**, *72*, 4149.
- (25) Chung, S. J.; Kim, K. S.; Lin, T. C.; He, G. S.; Swiatkiewicz, J.; Prasad, P. N.; *J. Phys. Chem. B* **1999**, *103*, 10 741.
- (26) Wokaun, A.; Lautz, H. P.; King, A. P.; Wild, U. P.; Ernst, R. R. *J. Chem. Phys.* **1983**, *79*, 509.
- (27) Weitz, D. A.; Garoff, S.; Hanson, G. D.; Gramila, T. J.; Gersten, J. I.; *Opt. Lett.* **1992**, *7*, 89.